Performance Assessment of Thermal Sensors for Hand Prostheses

Enrica Stefanelli, Marika Sperduti, *Graduate Student Member, IEEE*, Francesca Cordella, *Member, IEEE*, Nevio Luigi Tagliamonte, and Loredana Zollo, *Senior Member, IEEE*

***Abstract*—Amputees using prostheses have a loss of somatosensory functions that should be restored to ensure a more stable grasp, slippage prevention, and protection from unbearable stimuli. Several studies show the necessity of integrating temperature sensors in prostheses to restore thermal sensations. The performance of the used sensors is usually not accurately analyzed when integrated into a prosthesis and a systematic testing protocol is generally missed. This study aims to compare systematically and rigorously the performance of commercial temperature sensors when integrated into a prosthetic fingertip. Four thermal sensors were selected. An experimental setup and a systematic testing protocol for sensor assessment were devised. The sensors were inserted into a 3-D printed fingertip and different object temperatures were considered. Moreover, a silicone layer was added to simulate the presence of a cosmetic glove and various object-to-sensor inclination angles were tested to reproduce a realistic contact. The optimal sensor for integration into a prosthetic fingertip was identified through a statistical analysis of the obtained results. The infrared (IR) sensor was selected, as it exhibited an average rise time < 0.01 s and of 0.04 ± 0.2 s, with and without silicone, respectively, and a mean error (ME) of $3.3\ °C \pm 5.1\ °C$ and $4\ °C \pm 5.4\ °C$ with and without silicone, respectively. All the tested sensors encountered a degradation of performance when the fingertip was covered with silicone and positioned at the highest inclination. These observations emphasize the significance of utilizing the presented standardized method, to evaluate the performance of thermal sensors in a realistic environment.**

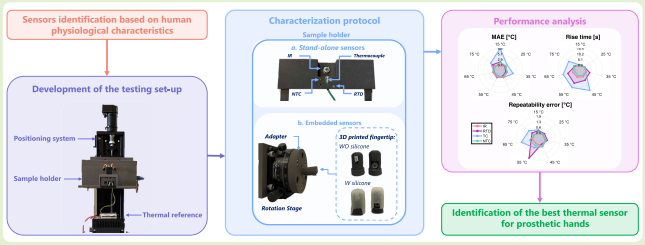

***Index Terms*— Characterization protocol, prosthesis thermal sensors, sensorized prosthetic hands.**

I. Introduction

THE human being is provided with a complex somatosensory system, which enables the sensation of touch, hot/cold, and pain thanks to various receptors, such as mechanoreceptors, nociceptors, and thermoreceptors [1]. These receptors are located in the human body's skin, with a high density in the hand compared with the rest of the body. The surrounding perception ensures the hand a stable grasp, slippage prevention, and also protection from painful stimuli [2].

Endowing a prosthetic hand with a somatosensory system similar to the human one could therefore enhance grasping performance and prosthesis acceptability [3]. Including in a closed-loop robotic prosthetic device the the capability of conveying thermal information to the user is an important aspect to artificially mimic the natural somatosensory system. Thermal sensors embedded in the prosthetic fingertips can detect objects temperature during manipulation. The data are encoded by means of specific algorithms able to restore the corresponding thermal sensation to the prosthesis user through sensory feedback techniques [4].

Furthermore, the thermal information could be useful to alert the prosthesis user of a dangerous situation or to control the prosthesis behavior to prevent possible damage to the prosthesis [5] and to the user [6], in case of contact with an object at an unbearable temperature.

Despite the expected improvement provided by temperature measures, there are still few examples of prosthetic hands incorporating temperature sensors in the literature. Stefanelli et al. [7] reported technical specifications to

Manuscript received 21 June 2024; revised 12 July 2024; accepted 15 July 2024. Date of publication 25 July 2024; date of current version 1 September 2024. This work was supported in part by the EU Commission through the Project SOMA: Ultrasound Peripheral Interface and In-Vitro Model of Human Somatosensory System and Muscles for Motor Decoding and Restoration of Somatic Sensations in Amputees under Grant H2020-FETOPEN-2019-899822 and in part by the Italian Institute for Labor Accidents (INAIL) Prosthetic Centre through WiFi-MyoHand under Grant CUP: E59E19001460005. The associate editor coordinating the review of this article and approving it for publication was Dr. Chun Zhao. *(Enrica Stefanelli and Marika Sperduti contributed equally to this work.) (Corresponding author: Enrica Stefanelli.)*

The authors are with the Laboratory of Advanced Robotics and Human-Centred Technologies (CREO Lab), Universitá Campus Bio-Medico di Roma, 00128 Rome, Italy (e-mail: e.stefanelli@unicampus.it).

Digital Object Identifier 10.1109/JSEN.2024.3431274

select a sensor to be integrated into a prosthetic hand's fingertips based on the human physiological characteristics in terms of response time and accuracy, and on physical features, such as object temperature range and size. In fact, the sensor's fast and accurate response is important for reproducing realistic sensory feedback, allowing a prompt reaction in case of unbearable temperature and informing the subject to make a decision about the grasping task to avoid the risk of injury [6]. In [8], a commercial thermistor was chosen and integrated into the fingertips of a low-cost prosthetic hand, in [9], a multisensor smart glove integrating commercial temperature and humidity sensors was designed, while in [10], a myoelectrical prosthetic hand, equipped with infrared (IR) thermometers, was designed to measure the temperature without the physical contact with the object. In [11], soft flexible thermistors were developed and integrated into a prosthetic device to test the performances, while in [4], active thermal skin made of platinum was used to reproduce temperature sensations in the phantom limb of an amputee. Moreover, in [12], a wearable tactile sensor for both temperature and contact force sensing was developed.

These studies emphasized the importance of temperature sensors in this context, but they leave some aspects of analysis still unexplored. For instance, in [8], the thermistor sensor was tested at a temperature of about 130 °C, resulting in an increase in the response time due to the silicone on the sensor. In [11], the instrumented fingertip was put in contact with a heated surface (170 °C) and a warm one (25 °C), resulting in a good discrimination of the two thermal conditions; in [12], the designed sensor was calibrated at a temperature of 25 °C and 60 °C, and then, it was integrated into the prosthesis and tested for three temperatures (25 °C, 50 °C, and 55 °C). Therefore, thermal sensors are currently selected based only on their stand-alone technical characteristics, without assessing the potential impact of the final application and real conditions on their performance. Thus, an important open issue is the employment of a systematic assessment to select thermal sensors, especially in realistic operative conditions, i.e., when integrated into prosthetic hands. In fact, external factors could influence the measures when using the sensors, particularly with critical object temperatures. Furthermore, the sensor placement as well as the presence of a cosmetic glove, used to make the prosthesis more similar to human hands [13], could impact both accuracy and response time. The latter factors could affect the naturalness and acceptability of the prosthesis in daily-life contests and discourage users from using it.

To overcome these important open issues that emerged from the literature, this article proposes the first systematic and rigorous protocol to compare the performance of temperature sensors when integrated into prosthetic fingers and operating in realistic conditions. To achieve this, several key methodological steps were followed. First, a specifically designed setup was developed to characterize thermal sensors in order to reproduce typical prosthesis operating conditions, allowing for an accurate assessment of sensor performance in a simulated real environment. Second, a testing protocol was defined taking into account several variables, including the change in the object temperature, the presence of a cosmetic glove and the position of the sensors in the fingers. This protocol guarantees the assessment of sensor repeatability, which is crucial as sensors must maintain consistent performance overextended periods, particularly when integrated into prosthesis for everyday use. Third, specific parameters and metrics were identified to evaluate the performance of the thermal sensors, to assess whether they can guarantee a response comparable to that of human hand receptors.

The adoption of the presented assessment protocol enables us to take into account application-specific aspects that can affect the performance of the sensors and which are typically neglected. This allows for a more reliable and accurate sensor selection process that is more consistent with the final application and with specific real working conditions. More specifically, we demonstrated how the protocol allowed the identification of the most suitable thermal sensors to provide accurate thermal feedback to the user in daily-life contexts, thereby increasing prostheses acceptability.

This article is structured as follows. In Section II, the sensors identification, the testing setup, the assessment protocol, and the performance comparison are described. The results, discussion, and conclusion are reported in Sections III–V, respectively.

II. Materials and Methods

The proposed study aims to compare the performance of temperature sensors to be integrated into a prosthetic hand.

The sensors were selected by taking into account technical specifications descending from the analysis of the characteristics of human physiology and daily-used objects. Then, the sensors were placed in contact with a temperature-controlled aluminum object (thermal reference), and the following conditions were tested: 1) stand-alone sensors: sensors performance is analyzed; 2) uncovered embedded sensors: sensors are integrated into a fingertip, varying the angular position of the sensor in the fingertip to measure the performance in several operative conditions; and 3) covered embedded sensors: the fingertip was covered with a silicone layer to assess the performance variations in the presence of a cosmetic glove. Although silicone has poor thermal conductivity, it was selected for this study since it represents the main material typically used for cosmetic gloves in commercial prostheses. Finally, a sensor was selected based on the performance analysis under the previously described conditions.

A. Sensors Identification

The main requirements for the identification of the temperature sensors are reported in Table I. In particular, the sensors must be small enough to fit inside the fingertips, so the human dimensions were taken as a reference [14], [15]; the sensors should have similar characteristics to the humans in terms of reaction time to thermal stimulus [16] and minimal thermal variation detectable by the humans [17]. Finally, the sensors should detect the temperature of all the daily life-used objects.

All the categories of commercial sensors were examined, such as IR, thermocouple (TC), negative temperature coefficient (NTC) thermistor, and resistance temperature

TABLE I
SPECIFICATIONS FOR THE SENSORS IDENTIFICATION AND ACTUAL TECHNICAL CHARACTERISTICS: (SIZE, RISE TIME, ME, AND TEMPERATURE RANGE)

	Technical specifications	NTC	TC	IR	RTD
Size [mm]	Width: [16 , 23] mm Height: [23 , 29] mm	ϕ 0.5 mm	ϕ 2.5 mm	8x6x12 mm^3	2x4 mm^2
Rise Time [s]	0.94	0.14 (in liquids)	3.96	0.22	0.14 (in liquids)
ME [°C]	±0.5	±0.2	±0.5	±0.5 [-40 , 125]	±0.1 [0 , 150]
Temperature range [°C]	[0 ,100]	[-40 ,125]	[-260 , 3600]	[-40 ,125]	[-50 ,600]

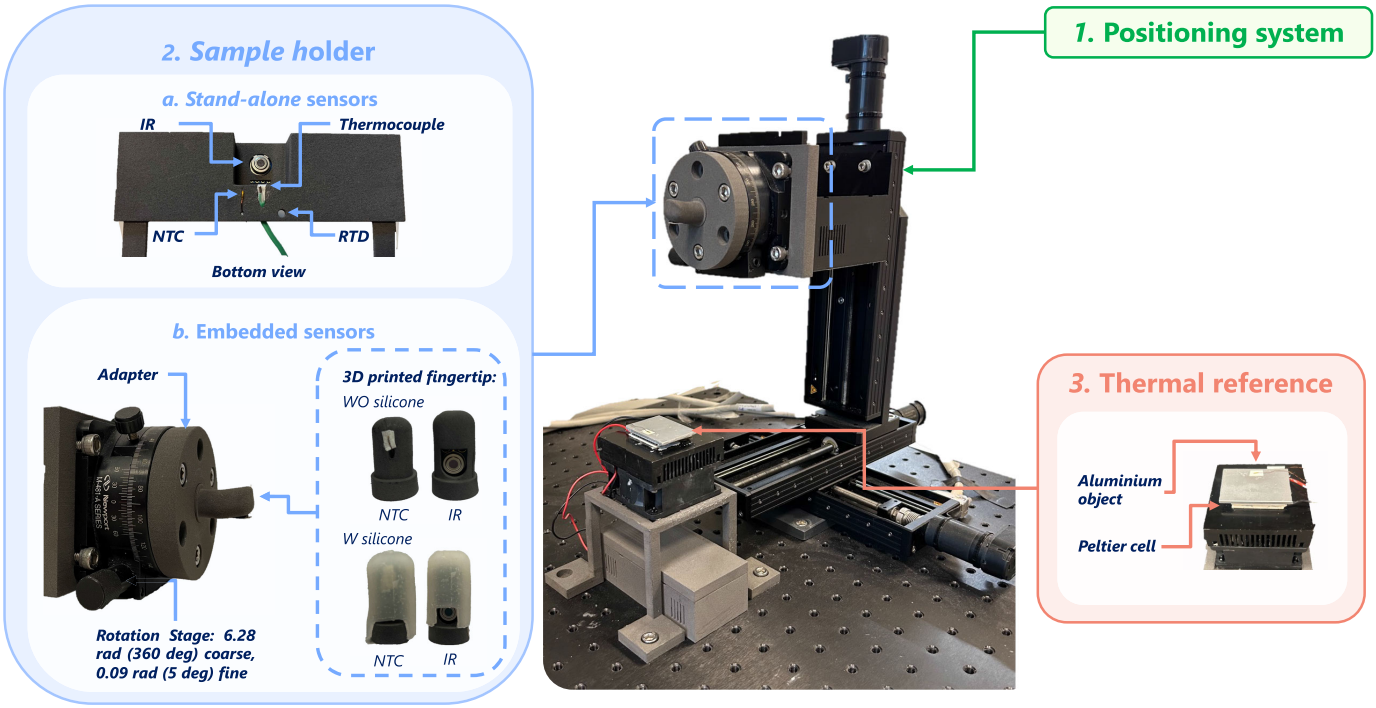

Fig. 1. Experimental setup. The three main components of the testing platform are reported: 1) positioning system; 2) sample holder; and 3) thermal reference. (a) Sample holder houses the four isolated sensors or (b) single sensor within the 3-D printed fingertip connected through an adapter to the rotational stage.

detector (RTD). The NTC and RTD are contact sensors whose resistance varies as a function of temperature. TC consists of two different conductors joined at one end and when this junction experiences a temperature change, it generates a voltage variation that can be acquired to determine the temperature. Finally, the IR is a contactless sensor which detects infrared radiation emitted by objects. Among the latter, the sensors with the closest match to the physiological human characteristics mentioned above were selected. Thus, the prosthesis device could behave more similar to a human, ensuring greater acceptability by the user. In particular, the MLX90614 (Malexis), 5-TC-KK-30 (Omega), GA10K3MCD1 (TE Connectivity), and PTFC102T1A0 (TE Connectivity) were analyzed. Moreover, the chosen sensors are all comparable in cost. All the chosen sensors were calibrated based on the recommendations from manufacturers' datasheets [18], [19], [20], and their technical characteristics are reported in Table I.

B. Testing Setup

The characterization procedure was carried on with the aid of a custom testbed, which was adapted from the one described in [21]. The adopted setup, reported in Fig. 1, is mainly made of three components.

1) *Thermal reference*, an aluminum object (10 × 10 × 2 mm^3) mounted over a Peltier cell. The object temperature is continuously controlled with a thermal controller (TEC).
2) *Positioning system*, a three-axis Cartesian positioning system that includes three linear stages (*PI VT-80*), with dc motors controlled by one multiaxis driver (PI C-884.4DC), whose main features are reported in Table II. It was used to approach in a gradual and controlled manner the thermal sensors to a temperature-controlled object.
3) *Sample holder*, an interchangeable holder mounted on the vertical axis of the positioning system, with two possible configurations depending on the tested condition of the characterization protocol. The two holder configurations are: 1) stand-alone sensors, where all the sensors are integrated in a 3-D printed structure and 2) embedded sensors, where each sensor is integrated into a 3-D printed fingertip.

TABLE II
MAIN FEATURES OF THE POSITIONING SYSTEM

	Linear stage PI VT-80
Stroke [mm]	150
Resolution [µm]	0.5
Max velocity [mm/s]	20

In configuration 1), the NTC, RTD, and TC sensors are positioned to be in contact with the temperature-controlled object. Since the IR sensor is based on a contactless technology able to read the underlying surface at an angle of 1.57 rad, it must be kept at a distance of 1 cm from the temperature-controlled object to allow optimal measurement of its temperature. The distance was calculated as the optimal value to read only the object temperature and not the surrounding area.
In configuration 2), the used fingertip was designed to be integrated in the prosthesis *IH2-Azzurra* (Prensilia, Pontedera, PI, IT). It was chosen since it has an open platform for research and is therefore easily exploitable to test different approaches. The sensors were placed on the surface of the fingertip, apart from the IR sensor which was enclosed into the fingertip due to its larger dimensions. In this configuration, a silicone cover, resembling the effect of a prosthesis glove, can be added. A silicone layer of 1 mm (consistent with the literature data [22]), was selected to match the thickness of the majority of cosmetic gloves. Nonetheless, it should be noted that different thickness values are expected to affect the sensors response since the higher the thickness the slower the heat conduction. The silicone layer was produced to cover the entire fingertip including the sensor, with the only exception of the IR, in correspondence to which a hole was added. This solution was adopted to avoid the IR would have measured only the temperature of the silicone and not of the underlying object due to its intrinsic feature of estimating the temperature only based on the emissivity. Moreover, in this configuration, the fingertip can be rotated with respect to the temperature-controlled object thanks to a *Newport 481-A Rotation Stage*, in order to validate the performance in several realistic hand-object contact.

4) *Acquisition board*, the data extracted from the thermal sensors were collected through a custom electronic board. The platform was synchronized with the electronic board in order to record the data as soon as the sensors went in touch with the object. The acquisition frequency was set to 10 Hz.

C. Characterization Protocol

The characterization protocol is divided into three different conditions: Stand-alone sensors, uncovered embedded sensors, and covered embedded sensors, as summarized in Table III.

1) Stand-Alone Sensors: In this condition, the protocol involves placing the sensor in contact with an object at different temperatures in the range [15, 75] °C with a step of 10 °C and repeating the experiment three times for each temperature value. The range was chosen to be consistent with the one selected in Section II-A. The contact time, (i.e., the duration of the acquisition when the sensor is in contact with the object) was set equal to 240 s to ensure that the sensor reaches the steady-state value. The same value must be set for the resting time, i.e., when the contact is absent, to allow the sensor to return to the room temperature.

TABLE III
CONDITIONS ADOPTED FOR THE PROTOCOL USED TO ASSESS THE PERFORMANCE OF THE SELECTED THERMAL SENSORS

	Stand-alone	**Covered embedded**		**Uncovered embedded**	
Temperature range [°C]	[15 , 75]	[15 , 75]	[15 , 55]	[15 , 75]	[15 , 55]
Temperature step [°C]	10	10	20	10	20
Repetitions	3	3	3	3	3
Angles range [rad]	–	0	[0.35 , 1.04]	0	[0.35 , 1.04]
Angle step [rad]	–	0	0.35	0	0.35

A statistical analysis was performed, as described in Section II-D.2, to identify the sensors that best replicate the chosen technical specifications. This choice was made to shorten the overall protocol, i.e., to reduce the number of subsequent tests described in the following.

2) Uncovered Embedded Sensors: The sensors selected in Section II-C.1 were integrated into the fingertip of a prosthetic device to evaluate how the performance could be influenced in a more realistic operative scenario. First, the sensor was positioned at 0 rad to the object, and the same protocol used in the first condition (Section II-C.1) was adopted. Then, the position of the sensors was changed with respect to the object in an angular range [0, 1.04] rad ([0, 60]°), with a step of 0.35 rad (20°), to simulate the possible contact configuration between the object and the fingertip.

The experiment was repeated three times for each temperature value in the range [15, 55] °C, with a step of 20 °C. Those temperatures were chosen because they elicit the range of sensations perceived by humans in everyday life (painful cold (15 °C), warm (35 °C), and painful heat (55 °C) [23]).

3) Covered Embedded Sensors: The experiments were carried out by putting a silicone cover over the sensor to assess how the presence of a glove can affect the measurements. Apart from that, the protocol was the same as the one used in Section II-C.2.

D. Performance Analysis

To evaluate the sensors performance, considering their integration into a prosthetic hand, the following indicators were selected as the most suitable: 1) mean error (ME), which needs to be comparable with the human's minimal thermal variation detectable; 2) rise time, to be compared with the human's reaction time to a thermal stimulus; and 3) repeatability error, to assess the reliability of the sensor. The same parameters were used to compare the selected sensors. Then, a statistical analysis was performed to select the best temperature sensors.

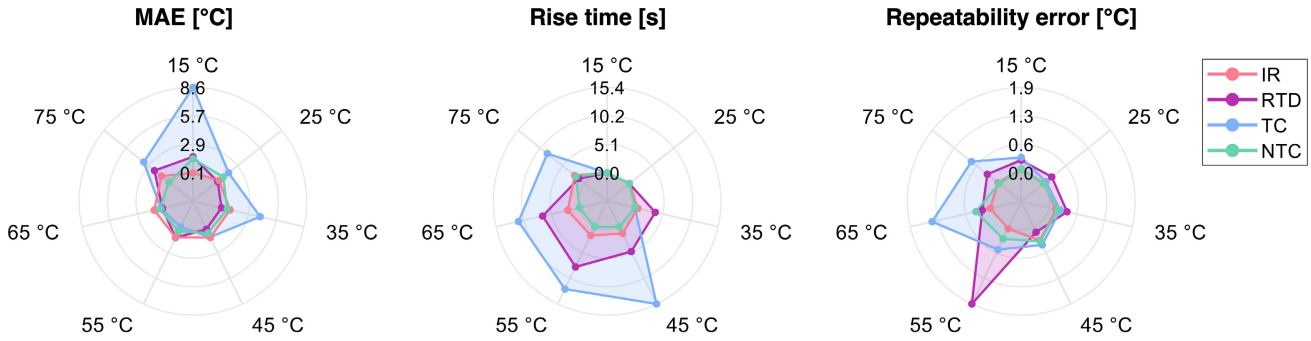

Fig. 2. MAE, rise time, and repeatability error of all the analyzed sensors (IR, NTC, RTD, and TC) at all the tested temperatures.

TABLE IV
MEDIAN VALUE (25 AND 75 PERCENTILE) OF THE ME AND RISE TIME FOR ALL THE ANALYZED SENSORS (IR, TC, NTC, AND RTD) AT ALL THE TESTED TEMPERATURES ARE REPORTED

	ME [°C]				Rise Time [s]			
Temperature [°C]	IR	NTC	RTD	TC	IR	NTC	RTD	TC
15	-0.10 (-0.14, -0.07)	1.79 (1.58, 1.79)	1.53 (1.47, 1.53)	-8.68 (-8.68, -8.41)	< 0.01	< 0.01	< 0.01	< 0.01
25	0.60 (0.597, 0.61)	0.51 (0.33, 0.51)	1.14 (1.14,1.14)	1.84 (1.79, 1.84)	< 0.01	< 0.01	0 (0.14, 0)	< 0.01
35	1.02 (1.00, 1.12)	-0.13 (-0.36, -0.4)	0.78 (0.70, 0.85)	-4.18 (-4.21, -4.01)	< 0.01	3.75 (2.60, 3.75)	0.55 (0, 1.87)	< 0.01
45	1.22 (1.15, 1.4)	-0.32 (-0.42, -0.32)	0.72 (0.62, 0.89)	1.13 (1.06, 1.40)	< 0.01	4.89 (4.78, 5.75)	1.29 (0, 1.36)	15.35 (15.01, 15.96)
55	1.30 (1.24, 1.27)	-1.27 (-2.00, -0.55)	0.48 (0.48, 0.70)	0.20 (-0.11, 0.32)	< 0.01	7.98 (4.18, 9.32)	1.69 (0, 1.72)	12.38 (11.38, 14.09)
65	1.21 (1.19, 1.25)	-0.44 (-0.48, -0.29)	0.54 (0.54, 0.85)	-0.70 (-1.05, 0.02)	0 (0, 0.15)	6.78 (6.46, 678)	2.13 (0, 2.17)	11.23 (9.46, 11.50)
75	1.28 (1.27, 1.29)	2.19 (2.03, 2.29)	0.34 (0.34, 0.34)	-3.61 (-3.81, -3.21)	2.03 (0.51, 4.53)	1.43 (1.36, 3.94)	2.35 (0, 2.37)	8.63 (8.39, 8.68)

1) Assessment Metrics: The indicators selected to assess the performance of the sensors in each of the three conditions described in Section II-B are as follows.

1) *ME [°C]*, to evaluate the error between the reference temperature (T_r) and the temperature measured by each sensor (T_m)

$$\mathrm{ME} = \sum \frac{1}{n} (T_r - T_m) \tag{1}$$

where n is the number of acquired samples. ME is calculated from the 90% of the length of the analyzed signal to the end (steady-state value), to ensure that only the steady-state value of the output is taken into account.

2) *Repeatability Error [°C]*, to identify the output variation in the repetitions when the conditions are constant, and the measurements are repeated within a short period of time. It is computed as follows:

$$R_e = |T_{m_{\max}} - T_{m_{\min}}| \tag{2}$$

where $T_{m_{\max}}$ and $T_{m_{\min}}$ are the average maximum and minimum temperature measurements [24]. The average is calculated considering the steady-state value.

3) *Rise time [s]*, the time taken for the signal to rise from one level (10%) to another (90%) of the last value. This variable was proposed since it is generally valid for all types of sensors, i.e., it is not only applicable to the ones that can be modeled as first-order systems [25].

2) Statistical Analysis: A statistical analysis was employed to evaluate the performance of the sensors in terms of ME and rise time. The analysis was performed both in the exclusion criterion, to select the two sensors to carry on in the protocol, and to finally select the most suitable temperature sensor. In this study, Wilcoxon's nonparametric statistical test was applied to the results. The significance level (p-value) was set at 0.05. In the first phase of the characterization protocol, the four sensors were compared adjusting the p-value at $0.05/n$, according to the Bonferroni correction, where n is 4.

III. RESULTS

The performance indicators (MAE, i.e. the absolute value of ME, rise time, and repeatability error) computed for the four selected sensors (IR, TC, NTC, and RTD) are shown in Fig. 2. For a more comprehensive analysis of the results, the median value, the 25 and 75 percentile of the ME and rise time are reported in Table IV. Furthermore, for the sake of clarity, the time-varying temperature for the four sensors is presented in the left part of Fig. 3. The ME for all the sensors at all the tested temperatures was in the range ±2.3 °C, except for the TC that presented the highest error among the sensors (−8.7 °C) when compared with the temperature-controlled object at 15 °C. The rise time of all the sensors had an increasing trend with the temperature, except for the TC that presented a peak of about 15.4 s in correspondence with the temperature of 45 °C. The rise time of the IR was < 0.01 s at all the temperatures with the exception of 75 °C (2.03 s).

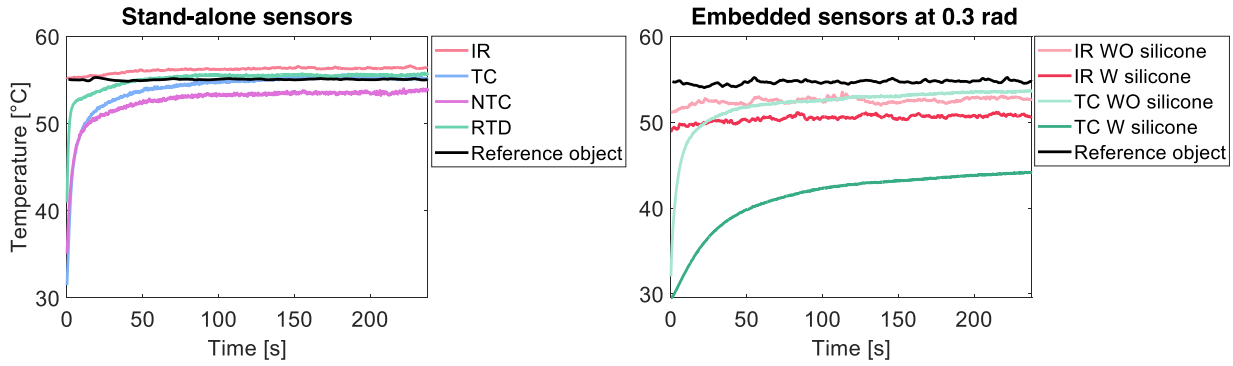

Fig. 3. Representative example of the time-varying temperature for the four stand-alone sensors at 55 °C (left) and for the embedded sensors with and without a silicone cover, with an inclination of 0.3 rad and 55 °C (right).

TABLE V
MEDIAN (25 AND 75 PERCENTILE) OF THE ME AND RISE TIME ARE REPORTED FOR THE IR AND NTC SENSORS, AT ALL THE TESTED TEMPERATURES, INTEGRATED IN A FINGERTIP WITHOUT (WO) AND WITH (W) A SILICONE COVER

	WO silicone				W silicone			
	ME [°C]		Rise Time [s]		ME [°C]		Rise Time [s]	
Temperature [°C]	IR	NTC	IR	NTC	IR	NTC	IR	NTC
15	-0.10 (-0.11, 0.03)	1.73 (1.73, 1.73)	< 0.01	< 0.01	0.15 (-0.21, 0.21)	1.64 (1.57, 1.63)	< 0.01	< 0.01
25	0.47 (0.43, 0.49)	1.42 (1.42, 1.42)	< 0.01	< 0.01	0.66 (0.63, 0.71)	1.46 (1.40, 1.46)	< 0.01	< 0.01
35	-0.41 (-0.46, -0.36)	1.13 (1.06, 1.20)	< 0.01	2.37 (2.32, 2.44)	0.44 (0.42, 0.49)	1.35 (1.13, 1.43)	< 0.01	7.40 (7.01, 9.59)
45	0.11 (-0.01, 0.23)	0.92 (0.92, 1.01)	< 0.01	4.35 (4.22, 4.51)	-0.49 (-0.70, -0.46)	-3.33 (-3.50, -3.33)	< 0.01	19.77 (18.54, 22.63)
55	0.23 (0.14, 0.50)	1.08 (0.96, 1.19)	< 0.01	5.48 (5.30, 5.77)	-1.25 (-1.61, -1.12)	-5.70 (-5.8, -5.70)	0 (0, 0.61)	26.96 (26.02, 27.82)
65	-0.73 (-1.03, -0.43)	1.58 (1.58, 1.58)	0 (0, 0.38)	6.04 (5.77, 6.37)	-2.11 (-2.42, -1.71)	-8.27 (-8.62, -8.03)	0.71 (0.18, 5.71)	33.05 (29.95, 34.45)
75	0.11 (0.06, 0.17)	1.67 (1.46, 2.09)	0.10 (0.03, 4.42)	6.75 (6.37, 6.76)	-3.85 (-4.03, -2.99)	-8.39 (-9.91, -8.24)	6.46 (2.30, 19.95)	29.97 (29.68, 37.02)

The repeatability error for all the sensors was lower than 1 °C, except for the RTD at 55 °C (1.9 °C) and the TC at 65 °C (1.4 °C). Thus, it appeared independent of the tested temperature. The statistical analysis was then carried out to compare the performance of the analyzed sensors, as described in Section II-D.2. The results showed that the RTD and TC sensors performed significantly worse than the other sensors; thus, only the NTC and IR were carried in the second condition of the protocol. More in detail, the NTC sensor was chosen since it presented the lowest ME (0.8 °C ± 0.4 °C in module) as well as for its statistical difference with the TC (p-value = 0.006) sensor. Moreover, the IR sensor was chosen since it was the one with the lowest rise time (0.36 s). Furthermore, it presented a statistical difference with all the other sensors (p-value = 0.0012 compared with the NTC, p-value = 0.001 compared with the TC, p-value = 1.3×10^{-4} compared with the RTD).

The ME, rise time, and repeatability error of the two selected sensors (NTC and IR) were analyzed once integrated into the 3-D printed fingertip with and without a silicone cover. The obtained results are shown in Table V without and with silicone and the global trend can be seen from Fig. 4. The ME value for both the sensors without silicone cover is ±2 °C for all the tested temperatures. On the other hand, when the fingertip was covered with a silicone layer, the ME showed an increasing trend with the temperature. Similar behavior could be observed also in the rise time for both sensors. This trend was accentuated when the sensors were covered with the silicone layer. The repeatability error for all the sensors at all temperatures was lower than 1 °C and presents an increasing trend that was higher with the silicone cover in both the sensors.

The performance of the two sensors integrated into the fingertip, taking into account the inclination angle with respect to the reference are reported in Table VI without silicone and Table VII with silicone. Moreover, a graphical representation is shown in Fig. 5. Furthermore, the time-varying temperature for the two embedded sensors, with and without the silicone layer, considering an inclination of 0.3 rad, is presented in the right part of Fig. 3. In both the analyzed sensors, with and without the silicone cover, the ME increased in module with the inclination angle for all the temperatures and it was significantly higher in correspondence of 55 °C. The rise time of the IR was almost <0.01 s for all the tested temperatures in both configurations. On the other hand, the NTC showed at 35 °C and 55 °C an increasing rise time with the angle and temperature. Finally, the repeatability error remained under 1 °C for both the sensors in all the tested conditions. The performance of the two sensors integrated into the fingertip was compared, showing a statistically significant difference between the rise time of the IR (<0.01 s) and of the NTC (12.4 ± 18.4 s in the module) integrated in the fingertip without the silicone cover (p-value = 6.9×10^{-9}). Moreover, a statistically significant difference (p-value = 0.0097) between

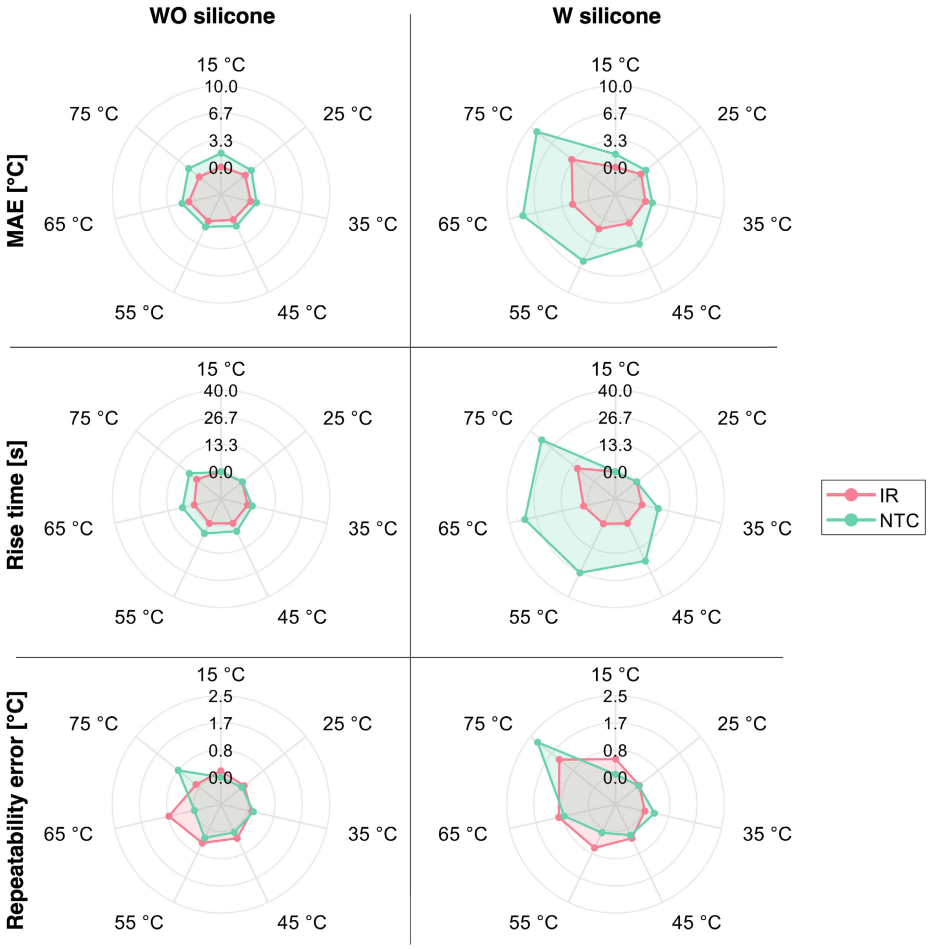

Fig. 4. MAE, rise time, and repeatability error reported for the IR and NTC sensors, at all the tested temperatures, integrated in a fingertip without (WO) a silicone cover on the left and with (W) a silicone cover on the right.

TABLE VI
MEDIAN (25 AND 75 PERCENTILE) OF THE ME AND RISE TIME ARE REPORTED FOR THE IR AND NTC SENSORS, AT DIFFERENT ANGLES COMPARED WITH THE REFERENCE (0, 0.35, 0.70, AND 1.04 RAD) FOR THREE TEMPERATURES (15 °C, 35 °C, AND 55 °C), INTEGRATED IN A FINGERTIP WITHOUT A SILICONE COVER

ME [°C]								
	IR				NTC			
Temperature [°C]	0 rad	0.35 rad	0.70 rad	1.04 rad	0 rad	0.35 rad	0.70 rad	1.04 rad
15	-0.10 (-0.11, 0.03)	-0.10 (-0.31, -0.04)	0.09 (0.08, 0.12)	0.53 (-0.63, 0.64)	1.73 (1.73, 1.73)	2.53 (2.53, 2.59)	4.18 (4.18, 4.44)	5.65 (5.58, 5.65)
35	-0.41 (-0.46, -0.36)	0.103 (-0.39, 0.24)	-3.68 (-3.77, -3.50)	-6.90 (-6.91, -6.68)	1.13 (1.06, 1.20)	0.15 (-0.06, 0.15)	-2.72 (-2.87, -2.66)	-6.78 (-6.78, -6.51)
55	0.23 (0.14, 0.50)	-2.14 (-2.28, -2.02)	-8.17 (-8.57, -8.05)	-17.38 (-17.7, -17.34)	1.08 (0.96, 1.19)	-1.23 (-1.33, -1.12)	-8.62 (-8.71, -8.62)	-18.33 (-18.49, -17.88)
Rise Time [s]								
	IR				NTC			
Temperature [°C]	0 rad	0.35 rad	0.70 rad	1.04 rad	0 rad	0.35 rad	0.70 rad	1.04 rad
15	< 0.01	< 0.01	< 0.01	< 0.01	< 0.01	< 0.01	< 0.01	< 0.01
35	< 0.01	< 0.01	< 0.01	< 0.01	2.37 (2.32, 2.44)	7.14 (6.95, 9.10)	13.20 (9.87, 13.39)	9.69 (9.41,16.88)
55	< 0.01	< 0.01	< 0.01	< 0.01	5.48 (5.30, 5.77)	13.80 (13.11, 16.72)	36.04 (34.02, 38.28)	50.47 (39.73, 78.16)

the ME of the IR (3.3 °C ± 5.1 °C in the module) and NTC (4.5 °C ± 4.9 °C in module) could be observed. On the other hand, for both the ME (IR: 4 °C ± 5.4 °C and NTC: 7.7 °C ± 5.6 °C) and the rise time (IR: 0.04 ± 0.2 s and NTC:

TABLE VII

MEDIAN (25 AND 75 PERCENTILE) OF THE ME AND RISE TIME ARE REPORTED FOR THE IR AND NTC SENSORS, AT DIFFERENT ANGLES COMPARED WITH THE REFERENCE (0, 0.35, 0.70, AND 1.04 RAD) FOR THREE TEMPERATURES (15 °C, 35 °C, AND 55 °C), INTEGRATED IN A FINGERTIP WITH A SILICONE COVER

ME [°C]								
	IR				NTC			
Temperature [°C]	0 rad	0.35 rad	0.70 rad	1.04 rad	0 rad	0.35 rad	0.70 rad	1.04 rad
15	0.15 (-0.21, 0.21)	-0.19 (-0.27, -0.10)	-0.20 (-0.26, -0.01)	0.36 (-0.08, 0.50)	1.64 (1.57, 1.63)	5.50 (5.44, 5.63)	6.96 (6.96, 6.96)	8.40 (8.34, 8.85)
35	0.44 (0.42, 0.49)	-1.13 (-1.27, -1.04)	-3.70 (-3.74, -3.65)	-7.22 (-7.34, -7.21)	1.35 (1.13, 1.43)	-2.86 (-2.86, -2.71)	-6.09 (-6.56, -5.89)	-5.79 (-5.86, -5.66)
55	-1.25 (-1.61, -1.12)	-4.44 (-4.48, -4.15)	-10.19 (-10.26, -10.15)	-18.38 (-18.47, -18.25)	-5.70 (-5.8, -5.70)	-10.78 (-10.87, -10.78)	-16.47 (-16.94, -16.31)	-20.21 (-20.35, -20.06)
Rise Time [s]								
	IR				NTC			
Temperature [°C]	0 rad	0.35 rad	0.70 rad	1.04 rad	0 rad	0.35 rad	0.70 rad	1.04 rad
15	< 0.01	< 0.01	< 0.01	< 0.01	< 0.01	< 0.01	< 0.01	< 0.01
35	< 0.01	< 0.01	< 0.01	< 0.01	7.40 (7.01, 9.59)	17.06 (12.39, 17.33)	27.94 (24.60, 41.98)	< 0.01
55	0 (0, 0.61)	0 (0, 0.46)	< 0.01	< 0.01	26.96 (26.02, 27.82)	47.16 (41.10, 48.00)	58.75 (56.10, 76.43)	51.20 (47.26, 57.47)

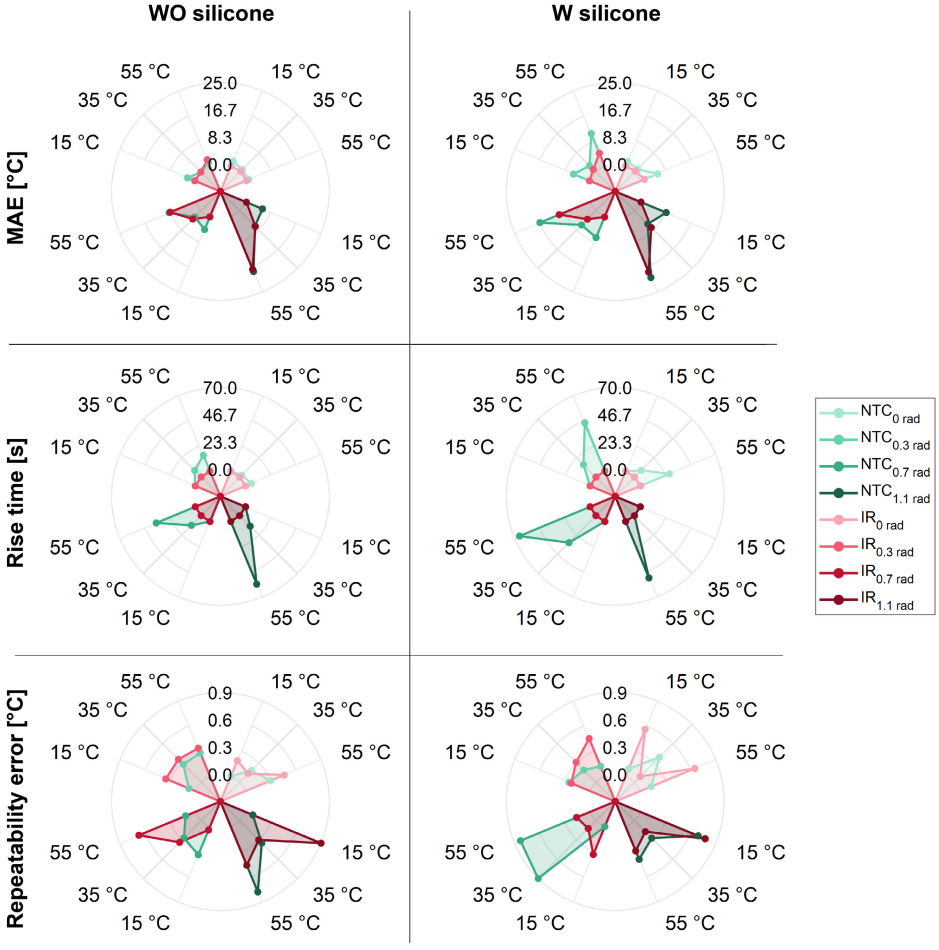

Fig. 5. MAE, rise time, and repeatability error for the IR and NTC sensors, at different angles compared with the reference (0, 0.35, 0.70, and1.04 rad) for three temperatures (15 °C, 35 °C, and 55 °C), integrated in a fingertip without (WO) a silicone cover on the left and with (W) a silicone cover on the right.

20.4 ± 23.4 s) a statistically significant difference between the sensors with a silicone cover was observed (ME: p-value = 1.9×10^{-4} and rise time: p-value = 8.1×10^{-7}).

IV. DISCUSSION

1) Comparison Analysis Among Sensors: This study aimed to compare the performance of multiple temperature sensors

in a comprehensive and repeatable way. Fig. 2 shows that the IR and NTC sensors presented better performance indicators in comparison with the other sensors in the study. As a matter of fact, the TC presented an irregular trend for all the performance indicators as well as multiple outliers (at 15 °C for the ME and at 45 °C for the rise time and at 65 °C for the repeatability). The NTC and IR sensors were selected to be tested once integrated into a 3-D printed fingertip as reported in Section II-C.2, since they presented the best ME and rise time, respectively, compared with the other sensors with a statistically significant difference. The performance of the sensors integrated in the fingertip considering an angle of 0 rad showed a low MAE and low repeatability error without the silicone cover, demonstrating their independence from the temperature, as reported in Fig. 4. On the other hand, the rise time without the silicone cover as well as the MAE, rise time, and repeatability error with the silicone cover, presented a growing trend with the temperature. Furthermore, this trend was more pronounced when using a silicone cover due to its insulating properties. Consequently, it took longer for the desired temperature to be reached, resulting in a longer rise time and a lower final temperature compared with the desired one. Therefore, the use of a custom silicone glove that did not cover all the NTC detection areas was suggested. The IR had lower MAE and rise time than the NTC when covered with the silicone layer since the IR was not completely covered by the silicone, as described in Section II-B. However, its performance was worse when the silicone cover was used since the IR could read the temperature of the silicone on the edge of the hole that included it.

Taking into account the impact of the inclination angle, as reported in Fig. 5, the MAE increased with the angle for both the sensors since the NTC started to detach from the object at an angle of 0.7 rad, and the IR detection area no longer solely captured the underlying object as the angle increased. Therefore, the measured temperature was influenced by the room temperature. For this reason, the MAE appeared independent of the silicone cover when an angle of 0.70 rad or greater was employed.

The rise time of the NTC was almost 0 s at 15 °C, regardless of the inclination angle, due to a low thermal gradient. On the other hand, for the other temperature values, the rise time of the NTC increased with the angle as the sensor was no longer in contact with the object. This caused the sensor to measure the air temperature, which was heated by the object, resulting in a slower trend of the sensor response and independence from the presence of a silicone cover. Moreover, the IR had always an instantaneous response. Finally, the low repeatability error indicated independence from the considered variables. Thus, it appears that the performance of the NTC is more dependent on the inclination angle than the one of the IR.

A statistical analysis was performed between the NTC and IR, showing a significant difference in both the ME and rise time regardless of the presence of the silicone cover.

The sensor selection should be pursued also based on other aspects besides strictly considering performance, such as functionality and operation. The two selected sensors have different working principles, which allow the temperature measurement to take place with (NTC) and without (IR) contact. Consequently, depending on the final application, one of the two options may be preferred over the other. The need for additional components, which increase complexity, may also affect the final choice since, for example, the NTC, differently from the IR, requires conditioning electronics.

2) Comparison Analysis With Human Somatosensory System: The temperature sensor to be embedded in a prosthetic hand should have similar characteristics to the human somatosensory system, as reported in Section II-A. Such an aspect is particularly important since it allows the prosthetic system to return information to the user promptly and to react in the case of painful situations. The results obtained by testing the selected sensors (IR, TC, NTC, and RTD) in the stand-alone test showed that only the NTC and IR are close to the human physiological characteristics (rise time: 0.94 s and ME: ±0.5 °C), the NTC ME was equal to 0.8 °C ± 0.4 °C in module, and the IR rise time was 0.36 s, with a statistical difference with the others sensors. In addition, analyzing the results obtained when the sensors were embedded in the fingertip, the IR exhibited an instantaneous rise time in all the analyzed configurations, comparable with the physiological reaction time (0.94 s). This aspect ensured a rapid response of the prosthesis in critical situations, such as contact with objects at extreme temperatures. The ME of the IR (3.3 °C ± 5.1 °C and 4 °C ± 5.4 °C with and without silicone cover) was the closest to the human one (±0.5 °C), allowing to accurately discriminate between painful (15 °C, 55 °C) and tolerable critical temperatures (35 °C). This is essential to ensure the safety and comfort of the prosthesis user, as it allows an appropriate reaction to potentially harmful situations. Furthermore, the IR sensor offers other advantages, such as its ability to measure temperature without physical contact with the object, which could reduce the risk of damage to the prosthesis and improve its durability. This is especially crucial in real-world scenarios, where the prosthesis must endure various environmental and usage conditions.

V. Conclusion

The present study, compared with the available literature, allowed a rigorous comparison, by adopting the proposed novel systematic protocol, between the performance of thermal sensors to be integrated into a hand prosthesis, taking into account realistic operative conditions. Multiple sensors were compared while they were in contact with objects at different temperatures. This is an essential step since the sensors performance is temperature-dependent, as illustrated in Fig. 2 and can be deeply observed from Table IV. This step allowed us to select both the IR and NTC sensors as they present good performance, comparable with the selected human somatosensory characteristics. The performance of the selected sensors was compared once integrated into a fingertip, as reported in Fig. 4 and Table V, and varying the orientation relative to the object, as shown in Fig. 5 and Tables VI and VII, considering in both case two configurations: with and without a silicone cover. The results show a worsening performance compared with the ones analyzed in the isolated sensors.

Therefore, the presence of a cosmetic glove in prosthesis (simulated by a silicone cover) and the orientation of the fingertip in a real scenario (simulated by varying the inclination angle), adversely influence the sensor's performance. Thus, the second phase of the presented protocol is essential for the identification of the thermal sensor. It allowed the identification of the IR sensor as the most suitable for prosthesis applications. The IR was selected to be integrated into the *IH2 Azzurra* prosthetic hand. However, the identification of the thermal sensor must take into account the demands of the ultimate application. In addition, the dimension of the prosthetic fingertip may be a further factor that can influence the sensor selection. The size of NTC and IR are well within the range needed for integration into most of the commercial prosthetic fingertips. These sensors can be easily adapted and scaled for different prosthesis sizes, ensuring that they meet the needs of users with varying anthropometric dimensions. For instance, the IR selected in this study incorporates conditioning electronics that increase its encumbrance, thus, for the integration in small fingertips, an IR with external electronics can be selected. The integration process is straightforward, and the performance remains reliable and accurate, making these sensors highly suitable for advanced prosthetic applications.

The proposed protocol represents a significant advancement over existing literature, since it ensures a more rigorous and systematic approach to selecting temperature sensors. Given the growing interest in the feedback of thermal information to prosthesis users, a proper selection of sensors can enhance the success of achieving this goal, particularly in everyday life contexts, not only in research. By addressing realistic conditions, this approach not only advances scientific understanding but also significantly improves the practical usability and, in perspective, the acceptance of prosthetic devices in daily life.

Future steps will be devoted to integrating the fingertips into the prosthetic hand and testing the system with healthy and amputee subjects.

REFERENCES

[1] Q. Hua et al., "Skin-inspired highly stretchable and conformable matrix networks for multifunctional sensing," *Nature Commun.*, vol. 9, no. 1, p. 244, Jan. 2018.

[2] T. Zhang, N. Zhang, Y. Li, B. Zeng, and L. Jiang, "Design and experimental evaluation of a sensorimotor-inspired grasping strategy for dexterous prosthetic hands," *IEEE Trans. Neural Syst. Rehabil. Eng.*, vol. 31, pp. 738–748, 2023.

[3] J. W. Sensinger and S. Dosen, "A review of sensory feedback in upper-limb prostheses from the perspective of human motor control," *Front. Neurosci.*, vol. 14, p. 345, Jun. 2020.

[4] F. Iberite et al., "Restoration of natural thermal sensation in upper-limb amputees," *Science*, vol. 380, no. 6646, pp. 731–735, May 2023.

[5] D. P. J. Cotton, P. H. Chappell, A. Cranny, N. M. White, and S. P. Beeby, "A novel thick-film piezoelectric slip sensor for a prosthetic hand," *IEEE Sensors J.*, vol. 7, no. 5, pp. 752–761, May 2007.

[6] R. M. Mayer et al., "Tactile feedback in closed-loop control of myoelectric hand grasping: Conveying information of multiple sensors simultaneously via a single feedback channel," *Frontiers Neurosci.*, vol. 14, p. 348, Apr. 2020.

[7] E. Stefanelli, F. Cordella, C. Gentile, and L. Zollo, "Hand prosthesis sensorimotor control inspired by the human somatosensory system," *Robotics*, vol. 12, no. 5, p. 136, Sep. 2023.

[8] D. Lanigan and Y. Tadesse, "Low cost robotic hand that senses heat and pressure," in *Proc. ASEE Gulf-Southwest Sect. Annu. Conf.*, Richardson, TX, USA, 2017, pp. 25–28.

[9] A. Polishchuk, W. T. Navaraj, H. Heidari, and R. Dahiya, "Multisensory smart glove for tactile feedback in prosthetic hand," *Proc. Eng.*, vol. 168, pp. 1605–1608, Jan. 2016.

[10] A. Badawy and R. Alfred, "Myoelectric prosthetic hand with a proprioceptive feedback system," *J. King Saud Univ. Eng. Sci.*, vol. 32, no. 6, pp. 388–395, Sep. 2020.

[11] A. Georgopoulou, L. M. Eckey, and F. Clemens, "A prosthetic hand with integrated sensing elements for selective detection of mechanical and thermal stimuli," *Adv. Intell. Syst.*, vol. 5, no. 10, Oct. 2023, Art. no. 2300122.

[12] Y. Wang, Y. Lu, D. Mei, and G. Qiang, "Development of wearable tactile sensor based on galinstan liquid metal for both temperature and contact force sensing," in *Proc. IEEE 16th Int. Conf. Autom. Sci. Eng. (CASE)*, Aug. 2020, pp. 442–448.

[13] C. Pylatiuk, S. Mounier, A. Kargov, S. Schulz, and G. Bretthauer, "Progress in the development of a multifunctional hand prosthesis," in *Proc. 26th Annu. Int. Conf. IEEE Eng. Med. Biol. Soc.*, Feb. 2004, pp. 4260–4263.

[14] S. Pheasant and C. M. Haslegrave, *Bodyspace: Anthropometry, Ergonomics and the Design of Work*. Boca Raton, FL, USA: CRC Press, 2018.

[15] B. Buchholz, T. J. Armstrong, and S. A. Goldstein, "Anthropometric data for describing the kinematics of the human hand," *Ergonomics*, vol. 35, no. 3, pp. 261–273, 1992.

[16] T. Jodai, M. Terao, L. A. Jones, and H.-N. Ho, "Determination of the thermal-tactile simultaneity window for multisensory cutaneous displays," in *Proc. IEEE World Haptics Conf. (WHC)*, Jul. 2023, pp. 230–236.

[17] J. C. Arezzo, H. H. Schaumburg, and C. Laudadio, "Thermal sensitivity tester: Device for quantitative assessment of thermal sense in diabetic neuropathy," *Diabetes*, vol. 35, no. 5, pp. 590–592, May 1986.

[18] *NTC Thermistor Sensors Performance*, document 02/2018, TE Connectivity, Schaffhausen, Switzerland, 2018.

[19] *Understanding RTDs*, document 07/2016, TE Connectivity, Schaffhausen, Switzerland, 2016.

[20] *A Basic Guide to Thermocouple Measurements*, document SBAA274A, Texas Instruments, Dallas, TX, USA, Sep. 2018.

[21] M. Sperduti, N. L. Tagliamonte, C. Casale, P. A. Netti, and L. Zollo, "A testbed for mechanical and thermal stimulation in studies of somatosensory functions," in *Proc. 8th Congr. Nat. Group Bioeng. (GNB)*, Padova, Italy, 2023, pp. 941–944.

[22] G. Smit and D. H. Plettenburg, "Comparison of mechanical properties of silicone and PVC (polyvinylchloride) cosmetic gloves for articulating hand prostheses," *J. Rehabil. Res. Develop.*, vol. 50, no. 5, p. 723, 2013.

[23] H.-N. Ho and L. A. Jones, "Modeling the thermal responses of the skin surface during hand-object interactions," *J. Biomech. Eng.*, vol. 130, no. 2, Apr. 2008, Art. no. 021005.

[24] M. Serge, T. Patrick, and F. Duquenoy, "Motion systems: An overview of linear, air bearing, and piezo stages," in *Three-Dimensional Microfabrication Using Two-photon Polymerization* (Micro and Nano Technologies), T. Baldacchini, Ed., Oxford, U.K.: William Andrew, 2016, pp. 148–167. [Online]. Available: https://www.sciencedirect.com/science/article/pii/B978032335321200008X

[25] N. Nise, *Control Systems Engineering*, 6th ed., Hoboken, NJ, USA: Wiley, 2011, ch. 4.

Enrica Stefanelli received the B.Sc. degree in industrial engineering and the M.Sc. degree in biomedical engineering from the Universitá Campus Bio-Medico di Roma, Rome, Italy, in 2018 and 2021, respectively, where she is currently pursuing the Ph.D. degree in bioengineering.

She is a part of the Research Unit of Advanced Robotics and Human-Centered Technologies (CREO Lab), Universitá Campus Bio-Medico di Roma. Her research is focused on upper limb prosthetic device control and sensorization, to optimize the prosthetic behavior in grasping and manipulation tasks by replicating the human somatosensory system.

Marika Sperduti (Graduate Student Member, IEEE) received the B.Sc. degree in clinical engineering from the Sapienza Universitá di Roma, Rome, Italy, in 2015, and the M.Sc. degree in biomedical engineering from the Politecnico di Torino, Turin, Italy, in 2018. She is currently pursuing the Ph.D. degree in bioengineering with the Universitá Campus Bio-Medico di Roma, Rome.

She was a Visiting Master Student with the Khademhosseini Laboratory, Harvard-MIT Division of Health Sciences and Technology (HST), Harvard Medical School (HMS) and its affiliated with the Brigham and Women's Hospital (BWH), Boston, MA, USA, in 2017. She is a member of the Research Unit of Advanced Robotics and Human-Centered Technologies (CREO Lab), Universitá Campus Bio-Medico di Roma. Her research activity is focused on developing and testing mechatronic and sensor-based technologies to restore realistic somatic sensations to amputees who use robotic prosthetic hands.

Francesca Cordella (Member, IEEE) is currently an Assistant Professor with Tenure Track (RTDb) at the Research Unit of Advanced Robotics and Human-Centred Technologies (CREO Lab), Universitá Campus Bio-Medico of Roma, Rome, Italy. She was and is involved in the role of a Co-Principal Investigator, the Project Manager, and the Scientific Manager of Work Package for more than 20 European and national projects in her fields of interest. She has authored or co-authored more than 100 peer-reviewed publications appeared in international journals, books, and conference proceedings. Her research interests are mainly in the field of biomechanics, biomedical robotics, human–machine multimodal interfaces, adaptive control strategies for collaborative robotics, vision-based approaches for motion reconstruction and human–robot interaction, psychophysiological assessment, closed-loop systems, and sensory feedback restoration.

Ms. Cordella has obtained the National Scientific Qualification for Second Level Professor in the Competition Sector 09/G2. She is a member of the Technical Program Committee and an Associate Editor for several international conferences, workshops, and journals.

Nevio Luigi Tagliamonte received the B.S., M.S., and Ph.D. degrees in biomedical engineering from the Universitá Campus Bio-Medico di Roma (UCBM), Rome, Italy, in 2006, 2008, and 2012, respectively.

He was a Visiting Ph.D. Student with the Biorobotics Laboratory, École Polytechnique Fédérale de Lausanne (EPFL), Lausanne, Switzerland, in 2011. He is currently a Tenured Track Assistant Professor of Bioengineering with UCBM, where he is a part of the Research Unit of Advanced Robotics and Human-Centered Technologies (CREO Lab). He collaborates as a Researcher with the Laboratory of Robotic Neurorehabilitation, Fondazione Santa Lucia, Rome. He has expertise in the fields of wearable robotics, biomechatronics, robots control, and physical human–robot interaction, compliant and variable impedance actuators, biomechanics, robot-aided neurorehabilitation, and user-centered assessment of robots interacting with humans. He participated in several national and European projects on wearable robotics and on neurorobotics and to industrial projects on biorobotics. Within these projects, he mainly worked on the development and testing of human-centered robotic technologies with a special interest in lower limb exoskeletons and in the assessment of exoskeleton-assisted walking in terms of biomechanical, clinical, physiological, and psychophysiological indicators. His research interests include design, development, and validation in clinical environments or biomedical robots, with specific attention to wearable systems for motor assistance and rehabilitation.

Loredana Zollo (Senior Member, IEEE) received the M.S. degree in electronic engineering from the Universita degli Studi di Napoli "Federico II," Naples, Italy, in 2000, and the Ph.D. degree in bioengineering from the Scuola Superiore Sant'Anna di Pisa, Pisa, Italy, in 2004.

She is a Full Professor of Bioengineering and the Director of the Master of Science in Biomedical at the Universitá Campus Bio-Medico di Roma (UCBM), Rome, Italy, where she is also the Director of the Laboratory of Advanced Robotics and Human-Centered Technologies (CREO Lab). She has been involved in more than 40 EU-funded and national projects in her application fields, such as the EU H2020/FET-Open/SOMA as a Project Coordinator and the EU H2020/ODIN and AIDE as a Scientific Coordinator for UCBM. She has authored or co-authored more than 160 scientific publications and six patents. Her research interests include rehabilitation and assistive robotics, biorobotics and bionics, human–machine interfaces, and collaborative robotics.

Open Access funding provided by 'Università "Campus Bio-Medico" di Roma' within the CRUI CARE Agreement